# Thermoelectric properties of skutterudite $CoSb_3$ thin films

M. V. Daniel,[1,a)] M. Lindorf,[2] and M. Albrecht[2]
[1]*Institute of Physics, Technische Universität Chemnitz, 09107 Chemnitz, Germany*
[2]*Institute of Physics, University of Augsburg, 86159 Augsburg, Germany*

(Received 1 April 2016; accepted 6 September 2016; published online 28 September 2016)

The thermoelectric properties of Co-Sb thin films with different Sb content and with a thickness of 30 nm were investigated with respect to the composition and the corresponding structural properties of these films. The films were prepared by molecular beam deposition either by codeposition on heated substrates or room temperature deposition followed by a post-annealing step. It was found that the prepared films exhibit bipolar conduction, indicated by a positive Hall constant and a negative Seebeck coefficient. The obtained results can be well explained by using the bipolar model, assuming heavy electrons and light holes, which was finally confirmed experimentally by the preparation of p- and n-type doped $CoSb_3$ thin films. Furthermore, variable range hopping was identified by temperature dependent transport measurements as dominant conduction mechanism at low temperatures. *Published by AIP Publishing*. [http://dx.doi.org/10.1063/1.4963111]

## I. INTRODUCTION

The material group of skutterudites, for instance, $CoSb_3$, are promising candidates for thermoelectric applications. Slack proposed their good thermoelectric efficiency already in 1994 within his concept of phonon glass-electron crystal materials[1,2] for which the thermal conductance is comparable to glass, and the electric properties are similar to a metal or semiconductor. An efficient thermoelectric material has therefore a low resistivity $\rho$, a high Seebeck coefficient $S$, and a low thermal conductivity $\kappa$, resulting in a high figure of merit $Z = S^2/\rho\kappa$. This is usually the case for materials with (i) complex unit cells, (ii) large atomic masses, (iii) low electronegativity differences of the individual atoms, and (iv) large carrier mobilities.[1,3] Slack recognized that all these requirements are fulfilled for skutterudites. However, their thermal conductivity, which is mainly based on phonons, is too large and he suggested filling the voids present in the skutterudite lattice structure by guest ions such as Yb to scatter the phonons and thus decrease the thermal conductivity.[3–6] Another way to improve $Z$ is the optimization of the power factor $S^2/\rho$ by controlled doping, which can be done by substitutions. In the case of $CoSb_3$, Co can be substituted by Ni (n-type) or Fe (p-type).[4,7,8]

A lot of work has been done for pure and filled skutterudite bulk materials and composites.[9–12] However, additional effects, occurring in thin film structures with a thickness in the nanometer range, could provide further improvement of the thermoelectric properties.[13–17] But only a few publications for skutterudite thin films exist, which are mainly dealing with the preparation and structural characterization of films with larger film thickness.[5,13,18–22]

In this work, the thermoelectric properties of 30-nm-thick Co-Sb films were investigated with respect to the deposition method, composition, and the corresponding structural properties of these films. Furthermore, the successful doping by filling with Yb (n-type) and by substitution of Co by Fe (p-type) is demonstrated and the influence on the transport properties is investigated.

## II. EXPERIMENTAL METHODS

Co-Sb thin films with different Sb content and with a thickness of 30 nm were codeposited in an ultra high vacuum (UHV) chamber with a base pressure of $1 \times 10^{-10}$ mbar by molecular beam deposition on thermally oxidized silicon $SiO_2$(100 nm)/Si(100) substrates (4″ wafers). Since the $SiO_2$ was amorphous, the films were not grown epitaxially. Two different approaches were used: (i) codeposition on heated substrates and (ii) deposition at room temperature followed by a post-annealing step. For the annealing process, the films were deposited on wafers and afterwards shortly exposed to air for breaking them into pieces. Different samples were mounted together, reintroduced, and post-annealed for 1 h in UHV. The used heating rate to reach the final temperature was 10 K/min. Further details of the deposition process can be found elsewhere.[23]

The composition and thickness of the as-deposited and annealed films were determined by Rutherford backscattering spectrometry (RBS). The structural phase formation in the films was investigated by x-ray diffraction (XRD). To increase the measured intensity, $2\theta$ scans with a fixed incident angle of 10° were performed.

The thermoelectric measurements were performed with home-built setups. The room temperature resistivity and the Hall constant were measured in van der Pauw geometry using spring loaded contacts. The Seebeck coefficient was determined by using a setup based on the work of Compans,[24] where the sample is placed over the slit of two heatable metal blocks. Each side of the sample is in contact with a single metal block. By heating one block, a gradient can be established in the sample, and by measuring the thermovoltage and the temperature gradient during the relaxation process by thermocouples, the Seebeck coefficient can be determined. The obtained values were corrected by the absolute Seebeck coefficients of the thermocouples.[25]

[a)]Electronic mail: marcus.daniel@physik.tu-chemnitz.de

The low temperature resistivity measurements were carried out with a cryostat using spring loaded contacts.

## III. RESULTS AND DISCUSSION

### A. Electric transport coefficients of Co-Sb thin films deposited at elevated temperatures

To investigate the influence of the composition of Co-Sb thin films on the thermoelectric properties, a series of films with an Sb content between 70 at. % and 80 at. % was codeposited on $SiO_2$(100 nm)/Si(100) substrates at three different substrate temperatures, 175 °C, 200 °C, and 230 °C. From previous studies, it is known that the range, where single phase skutterudite films are formed, is very narrow and becomes even more narrow with higher substrate temperature.[23] Exemplarily, an XRD ($2\theta$) scan of a single phase $CoSb_3$ film with an Sb content of 76 at. % deposited at 230 °C is shown in Fig. 1 (top), where only peaks of the skutterudite phase can be found. Additionally, it was found that the grain size decreases with the substrate temperature from 550 nm (175 °C) to 20 nm (230 °C).[23]

The thermoelectric properties measured at room temperature are summarized in Figs. 2(a)–2(e) as a function of the Sb content for the different substrate temperatures during deposition. The single phase composition ranges are marked in Fig. 2(e) for the different deposition temperatures in dependence of the Sb content. Since the sample series deposited at 200 °C and 230 °C show basically the same behavior, these series will be discussed first.

In Fig. 2(a), the dependence of the resistivity $\rho$ on the composition of the deposited Co-Sb films is shown. For deposition temperatures of 200 °C and 230 °C, a maximum in resistivity is observed close to an Sb content of 75 at. %. This value corresponds to the exact stoichiometry of the $CoSb_3$ skutterudite phase, and therefore, films with a low number of crystal defects are expected. Since the $CoSb_3$ phase is semiconducting, the largest resistivity is observed for these films. If the composition differs from this value, vacancies or additional atoms on interstitial lattice sites act as n-type dopants and increase the charge carrier density $n$ (lower Hall constant $R_H$),[18,19,26] resulting also in a lower resistivity. Savchuk *et al.*[19] described n-type doping in Sb deficient films due to Co atoms on interstitial sites or the presence of Sb vacancies. Co substituting the Sb sites is not expected, since the formation energy is relatively large. Smalley *et al.*[18] reported for annealed Sb deficient $CoSb_3$ films also n-type doping due to defects. For Sb rich samples, they found an incorporation of Sb into the voids yielding n-type, which overcompensates the p-type doping due to Co vacancies.[18] For larger deviations from the ideal composition of 75 at. %, the concentration of such defects increases further, thus degeneration should occur and metallic-like behavior should be observed. If additional phases are formed for even larger deviations of the Sb content from the compensated semiconducting state, these phases could provide additional electronic current paths that short-circuit the semiconducting phase. In this regard, it was reported that the charge carrier density and the Seebeck coefficient decrease due to the formation of such impurity phases.[4]

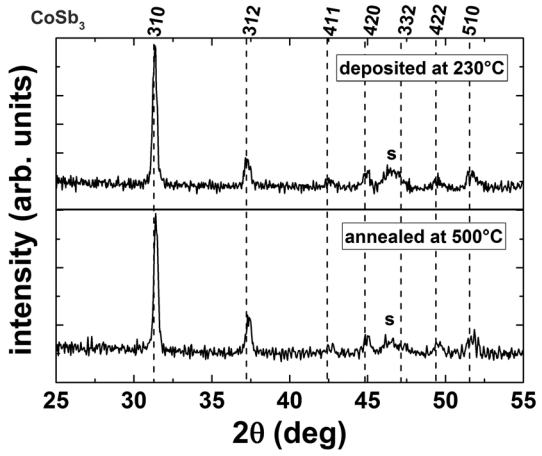


FIG. 1. XRD ($2\theta$) scans of 30 nm thick Co-Sb films on $SiO_2$(100 nm)/Si(100) substrate with an initial Sb content of 76 at. %: (top) film deposited at a substrate temperature of 230 °C; (bottom) film deposited at room temperature and post-annealed at 500 °C. Only peaks corresponding to the $CoSb_3$ skutterudite phase can be detected, which are marked by the corresponding indices. Substrate peaks are labeled with s.

The Hall constant $R_H$ was determined to confirm the doping effect due to vacancies or interstitials. It is positive for all films deposited at 200 °C and 230 °C, indicating dominant p-type conduction (Fig. 2(c)). This is in agreement with the literature, where $CoSb_3$ is mainly described as p-type semiconductor.[11,19] As expected, a maximum of $R_H$ was found for almost stoichiometric films with an Sb content of around 75 at. %, where the maximum of $\rho$ was also observed (Fig. 2(a)). In summary, the decrease of both $R_H$ and $\rho$ for non-stoichiometric films can be related to self-doping by defects given by vacancies or additional atoms on interstitial lattice sites.

Samples with a high resistivity and a large Hall constant usually show a large absolute value of the Seebeck coefficient. Indeed, the measurements also reveal a maximum of $|S|$ for an Sb content of about 75 at. % as shown in Fig. 2(b). However, the obtained Seebeck coefficients have negative sign and reach low absolute values ($\sim -20$ $\mu$V/K) at room temperature compared to typical values of 150 $\mu$V/K for p-type and $-300$ $\mu$V/K for n-type $CoSb_3$ reported in the literature.[11,12] The observed negative sign of the Seebeck coefficient is in disagreement to the positive sign of the Hall constant, indicating that two types of charge carriers (electrons and holes) contribute to the transport properties in the Co-Sb thin films. Since electrons and holes compete for the Seebeck effect, the low absolute values can be explained. The resulting power factors $S^2/\rho$ are thus very small and nearly independent on composition (Fig. 2(d)). The observation of different signs of Seebeck coefficient and Hall constant due to bipolar conduction was, for instance, also reported by Kitagawa *et al.*[27] for Ni doped $CoSb_3$.

Furthermore, a correlation between the discussed thermoelectric properties and the structural properties can be found. The range of the Sb content is where single phase skutterudite films are obtained (Fig. 2(e)) and the observed extrema of the transport coefficients are always observed within this range. Since the single phase range is smaller for films deposited at 230 °C, the corresponding extrema are

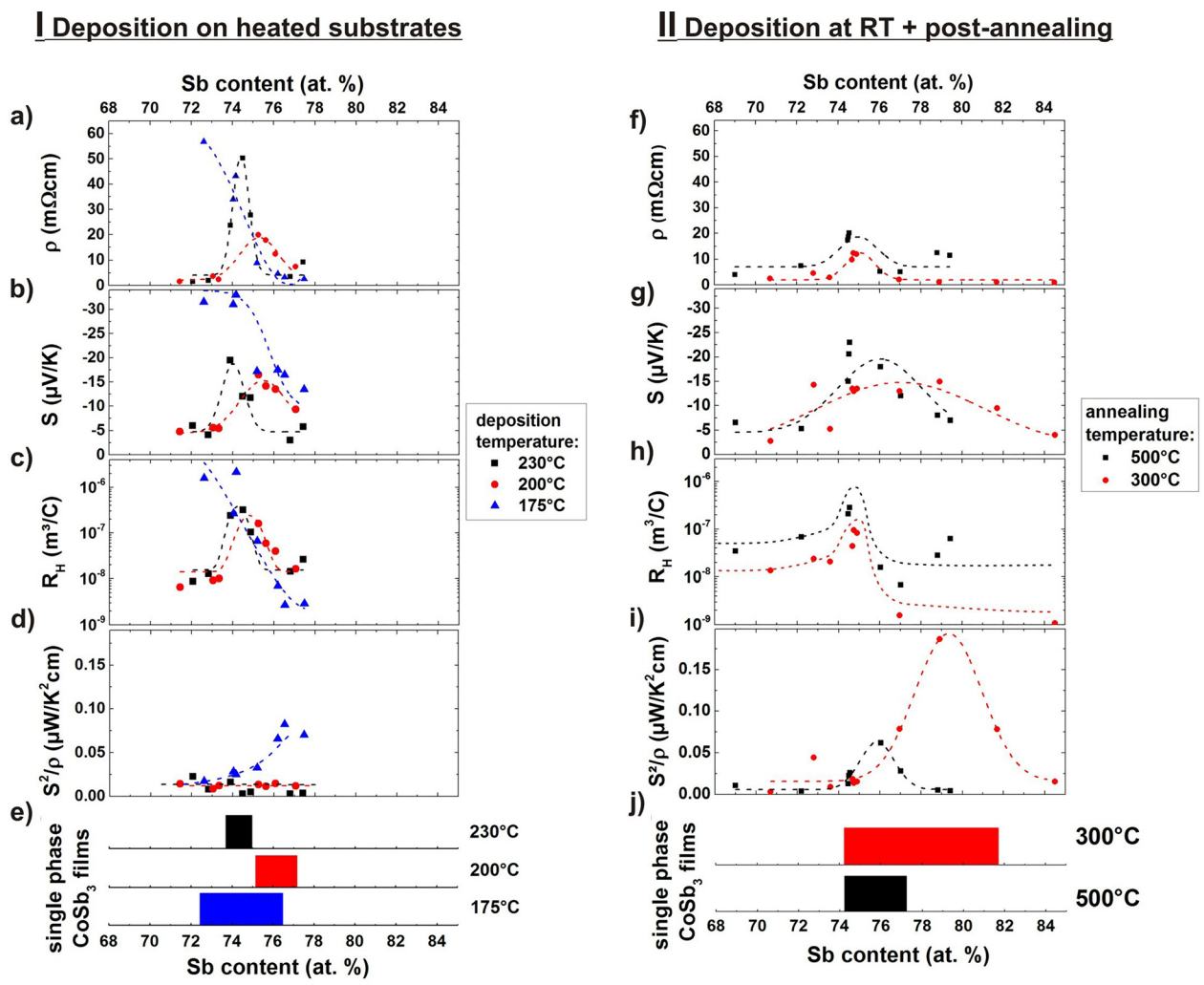


FIG. 2. Thermoelectric properties in dependence on the Sb content for Co-Sb films prepared with different approaches: I: deposited at different substrate temperatures [(a)–(e)] and II: deposited at room temperature (RT) followed by post-annealing [(f) – (j)]. The resistivity $\rho$, the Seebeck coefficient $S$, the Hall constant $R_H$, and the power factor $S^2/\rho$ are presented. Additionally, the bar diagrams at the bottom indicate the composition range for single phase skutterudite films. The dashed lines are only a guide to the eye.

also sharper. As already mentioned, a maximum of $S$ for single-phase films is also expected.[4,28] The observed differences in the transport parameters between the sample series deposited at 200 °C and 230 °C (230 °C: higher resistivity, higher Seebeck, and higher Hall constant) are mainly caused by different microstructures (e.g., smaller grain size for films deposited at 230 °C).[23]

The films deposited at 175 °C reveal a different behavior. While films deposited at higher deposition temperatures exhibit the $CoSb_2$ phase for an Sb content lower than 74 at. % and the Sb phase for an Sb content larger than 77 at. %, leading to a drastic drop in resistivity, in this sample series, the $CoSb_2$ phase does not form.[23] Thus, only a steady decrease in resistance can be found for Sb rich samples. Films with lower Sb content than 75 at. % do not exhibit this drop. Down to an Sb content of 72 at. %, single phase skutterudite films are obtained, and for these films, the maximum resistivity is observed. This process is not fully understood. Sb vacancies as well as Co interstitials should dope the material, and the resistivity should be reduced even though no $CoSb_2$ is formed.[19,26] Nevertheless, the absolute value of the resistivity is in the same order of magnitude as found for the other sample series deposited at higher temperatures. By increasing the Sb content, the material gets doped and the resistivity decreases. This is confirmed by the results obtained for the Hall constant, which is the largest for low Sb contents and decreases by doping of the material with increasing Sb content. It is also positive, while the Seebeck coefficient is negative. $|S|$ is larger than for the series deposited at higher deposition temperatures, and the maximum absolute value achieved for the Sb deficient samples is about $-33\,\mu$V/K. The reason for the larger Seebeck coefficient might also be caused by different grain sizes and structural differences.[23] The calculated power factor increases with increasing Sb content, reaching values up to $\sim 0.08\,\mu W/K^2\,cm$. The decrease in resistivity with higher Sb contents is steeper than the one observed for the Seebeck coefficient, and therefore, both properties do not fully compensate each other.

To obtain further insights into the origin of the bipolar conduction mechanism, low temperature resistivity measurements were performed for the films deposited at 230 °C. The obtained curves are shown in Fig. 3(a). It can be seen that all films exhibit a negative slope typical for semiconductors. For the lowest Sb content, the resistivity is nearly constant.

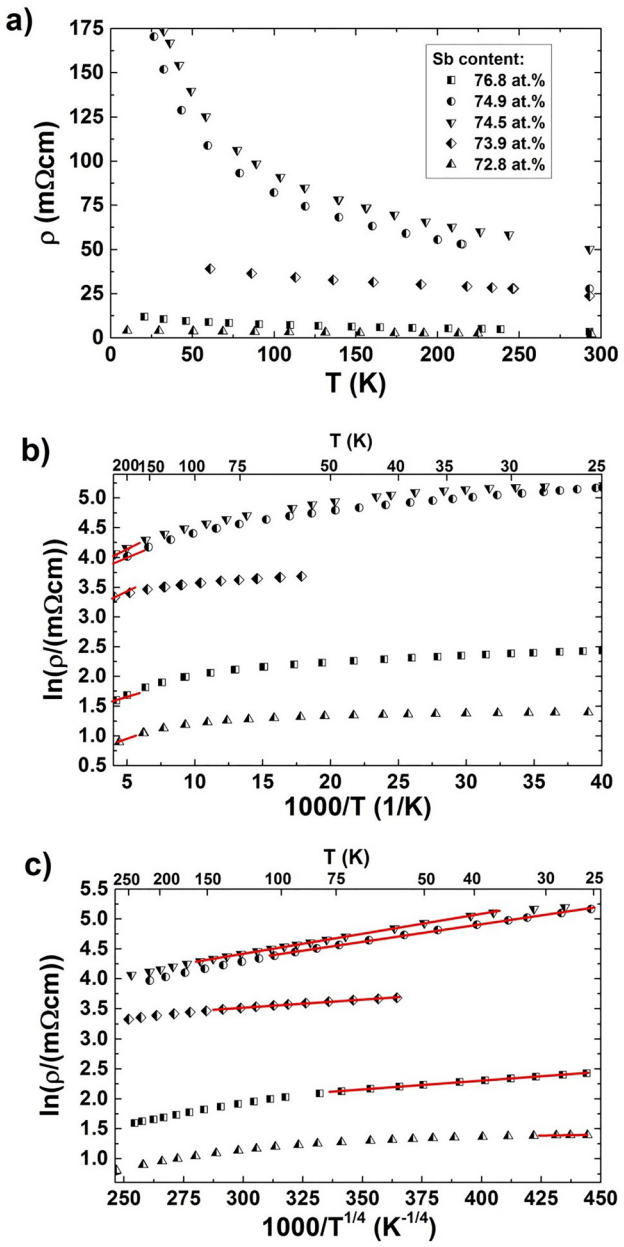


FIG. 3. (a) The temperature dependence of the resistivity $\rho$ for Co-Sb films with different Sb content deposited at 230 °C. For an Sb content close to 75 at. %, semiconducting behavior is observed. (b) The logarithm of $\rho$ in dependence on $T^{-1}$ for Co-Sb films with different Sb content deposited at 230 °C. For temperatures below 200 °C, no linear behavior is observed or only in a very narrow temperature range. Above 200 K, a constant slope is approached (red lines). (c) The logarithm of $\rho$ in dependence of $T^{-1/4}$ for Co-Sb films with different Sb content deposited at 230 °C. A linear dependence indicates variable range hopping (VRH). The corresponding temperature regimes are much larger and fitted by a linear function (red lines). Note that the actual density of data points during the measurement was much larger.

The deviation from the stoichiometric Sb content of 75 at. % yields a lot of defects and the formation of different phases, both resulting in large charge carrier densities, degeneration, subband formation, or additional current paths. With increasing Sb content, the number of defects is decreasing first, and thus, the resistivity and also the relative change with temperature increases. The most pronounced semiconducting behavior is indeed found for an Sb content of around 75 at. % as expected. For even larger Sb contents, the number of defects increases again, the material gets doped, and the resistivity decreases. Finally, the sample with an Sb content of 76.8 at. % reveals again a nearly temperature independent resistivity, which is typical for highly doped or degenerated semiconductors. Note that it is possible to cover the whole range of resistivity curves reported in the literature for $CoSb_3$ thin films only by slightly varying the composition.[4,19,28,29]

The bandgap width $E_g$ or the existing excitation levels are usually investigated by plotting the logarithm of $\rho$ over $T^{-1}$ and performing a linear regression to determine the corresponding slope $a$

$$E_g = 2k_B a,$$

where $k_B$ is the Boltzmann constant. This formula is valid for non-degenerated semiconductors and pure phonon scattering, which might only be the case for the films with the highest resistivity and for temperatures above 200 K. Above this temperature, the curves are indeed approaching a linear slope (see Fig. 3(b)) and a bandgap width of about 20 meV can be extracted. This is relatively low in comparison to values reported in the literature, which are usually larger than 50 meV.[9,10,13] Furthermore, the onset of intrinsic excitation is reported in a temperature range between 300 K and 600 K, and a linear dependence is usually not observed in the temperature range investigated here.[11] Another possibility to explain the low value is the onset of charge carrier excitation from an impurity band as suggested by Dyck *et al.*[30] and supported by the multi-band calculations of Kajikawa.[31] They have reported excitation energies in the same order of magnitude. Furthermore, Kajikawa[32] derived a decrease of the excitation energy with increasing charge carrier concentration in this impurity band. However, to proof the presence of an impurity band and to extract its bandgap, Hall and resistivity measurements at higher temperatures are needed.

Below a temperature of 200 K, no linear behavior can be observed in the plots of $\ln(\rho)$ over $T^{-1}$ (Fig. 3(b)), and the resistivity data cannot be explained by band excitation. At low temperatures, it is typical for highly doped semiconductors with small band gaps to find variable range hopping (VRH) based on localized electrons.[33–35] The theory predicts a linear dependence for $\ln(\rho)$ over $T^{-1/4}$.[33] These plots are shown in Fig. 3(c). All samples exhibit at low temperatures a linear behavior as indicated by the additionally plotted linear fits (red). Towards higher temperatures, the curve gets more and more bended and the absolute value of the slope increases steadily. The temperature $T_{dev}$, at which the change from linear to the more bended curve occurs, differs for the different compositions and a maximum of about 160 K is obtained for films close to the stoichiometric Sb content of 75 at. %. These films exhibit the lowest number of defects and thus the lowest doping level is expected. If the defect/doping concentration is small, the number of excitation levels in the gap is smaller and the number of charge carriers, which can be excited at a certain temperature into the conduction band, is also smaller. The energy available at low temperature might therefore be not enough to excite charge carriers into the conduction band and between the doping

states VRH can occur up to higher temperatures. The characteristic temperature $T_0$[33] of this samples is 2015.1 K and was extracted from the slope of the curve. If the defect/doping concentration is increased by deviations from the stoichiometric Sb content, more and more impurity states might be generated in the gap and the probability to excite charge carriers to the conduction band is increased for these samples, resulting in a lower $T_{dev}$. For even higher doping, the formation of an additional subband in the gap could occur and no VRH is observed at all. The formation of such a subband is likely for a narrow bandgap semiconductor like $CoSb_3$; however, it is very complicated to investigate. VRH in $CoSb_3$ and Ni-doped $CoSb_3$ bulk samples was also observed by Dyck *et al.*[30] and Sun *et al.*[36] However, they have obtained a much lower transition temperature of 50 K or lower, which is comparable to typical values reported in the literature.[37,38] In our case, the presence of the VRH would also support the existence of an impurity band corresponding to the low excitation energy of 20 meV.

### B. Electric transport coefficients of post-annealed Co-Sb films

Co-Sb films with Sb contents between 69 at. % and 86 at. % were codeposited at room temperature on $SiO_2$(100 nm)/Si(100) substrates and post-annealed to investigate the thermoelectric properties in dependence on the Sb content. One series was annealed at $T_A = 300\,^{\circ}C$ and the other at $T_A = 500\,^{\circ}C$. The structural properties of post-annealed films differ significantly compared to films deposited at elevated temperatures, resulting also in pronounced differences of the thermoelectric properties. The composition range, where only the skutterudite phase is formed, is larger for post-annealed films.[23] This is illustrated in Fig. 2(j) by the colored bars for both annealing temperatures, and additionally, an XRD ($2\theta$) scan of a single phase film annealed at 500 °C is shown in Fig. 1 (bottom). Furthermore, all post-annealed films are smoother over the entire composition range compared to films deposited at elevated temperatures, and their grain size is also much larger (1 $\mu$m–10 $\mu$m).[23]

The determined thermoelectric properties are summarized in Figs. 2(f)–2(i) in dependence on the Sb content for the two annealing temperatures of 300 °C and 500 °C. Note that the Sb content was measured by RBS after the annealing process.

The resistivity exhibits for both annealing temperatures a peak for an Sb content of about 75 at. % as also observed for films deposited at elevated temperatures. However, the width of the resistivity peak is for annealed films much narrower than the composition range, where single phase skutterudite films are observed (Figs. 2(f) and 2(j)). This range lasts for instance up to an Sb content of 82 at. % for films annealed at 500 °C, while the resistivity drops already at a value of 76.5 at. %. The absolute resistivity values of the annealed samples are smaller compared to the measured values for films deposited at elevated temperatures (compare Figs. 2(a) and 2(f)) and might be related to the larger grain size (less grain boundary scattering) and smoother surface (less surface scattering) of the post-annealed films. The Hall measurements indicate indeed an increased scattering, since there is no significant difference of the Hall constant between the films of both preparation types. A maximum around 75 at. % Sb is observed for the annealed films (Fig. 2(h)), and the absolute values are even slightly increased compared to films deposited at elevated temperatures (Fig. 2(c)). Therefore, the decrease of resistivity has to be attributed to a higher mobility (less scattering).

The Seebeck coefficients are comparable to the values found for films deposited at elevated temperatures and also reveal a negative sign contrary to the positive Hall constants, which is again an indication for bipolar conduction. The absolute value of $S$ is less sensitive to the Sb composition than the resistivity, and a broad maximum is observed (73 at. %–80 at. %, Fig. 2(g)). It is suggested that the increase is strongly correlated to the formation of single phase skutterudite films. Since single phase skutterudite films can be observed for post-annealed films in a much broader composition range, the maximum of $S$ is also much broader than the one observed for films deposited at elevated temperatures. Impurity phases can yield a decrease of the Seebeck coefficient, as already mentioned in Section III A.[4,28] The enlarged $S$ for single phase films was less apparent for films deposited at elevated temperatures, since the respective composition range of single phase films is as narrow as the peak width of the resistivity is caused by self-doping due to a non-stoichiometric Sb content. Therefore, the maxima in Seebeck coefficient and resistivity could be both explained by a change in the Sb content and thus by self-doping (Fig. 2).

The different characteristic of $S$ and $\rho$ with respect to the Sb content influences the power factor $S^2/\rho$ strongly. The peak of the Seebeck coefficient is therefore not fully compensated by the resistivity peak (as found for the films deposited on heated substrates), and thus, the power factor shows a pronounced maximum between 75 at. % and 82 at. % Sb (Fig. 2(i)). The power factor of the post-annealed samples is additionally improved by the lower resistivity due to less scattering at the grain boundaries and the surface. The maximum position is shifted for the different annealing temperatures, and larger values up to 0.2 $\mu W/K^2$ cm can be achieved for films post-annealed at 300 °C.

By comparing the results for different annealing temperatures, it was found that a higher annealing temperature yields samples with a larger resistivity and a larger Seebeck coefficient. It is suggested that this increase is caused by a better crystallinity with less defects like Sb on interstitial positions.[18,23,39] The healing of defects at higher temperatures causes less parasitic doping states, and hence, a lower charge carrier density is achieved, which results in an increase in resistivity and Seebeck coefficient. However, the overall power factor is smaller.

Additionally, low temperature measurements were performed for the single phase skutterudite films. In Fig. 4(a), an overview of the temperature dependence of the resistivity for the samples annealed at 300 °C is shown. The samples, showing the largest resistivity at room temperature, reveal the largest resistivity over the entire temperature range as well as the largest absolute change. This supports the results obtained for films deposited at elevated temperatures. The strongest semiconducting behavior is again found for films with an Sb

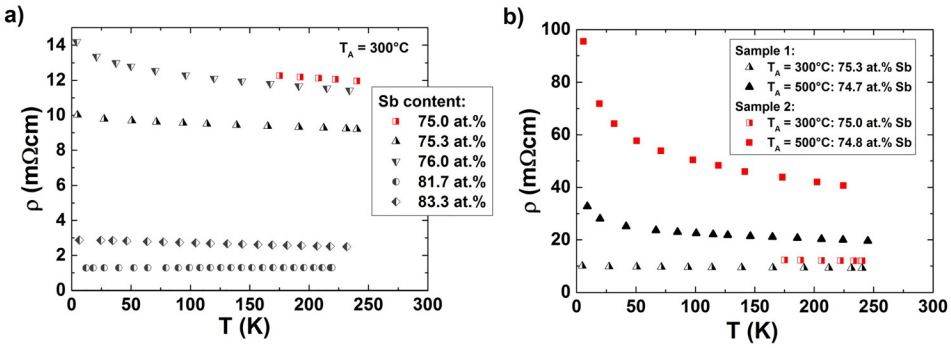


FIG. 4. Temperature dependence of the resistivity for post-annealed Co-Sb films: (a) for films with different composition annealed at $T_A = 300\,^{\circ}\mathrm{C}$ and (b) for two selected samples, demonstrating the resistivity change due to annealing at different temperatures (300 °C and 500 °C).

content close to the stoichiometric Sb content of $CoSb_3$. If the Sb content is lower or higher than 75 at. %, the resistivity and the temperature coefficient drop as described before.

Furthermore, the influence of the used annealing temperature on the temperature dependence of the resistivity is shown for two samples with an Sb content of around 75 at. % in Fig. 4(b). The defect healing induced by annealing at higher temperatures decreases the charge carrier density and lowers the amount of impurity states distorting the band gap. Thus, a stronger temperature dependence of the semiconducting-like resistivity is obtained. Note that the obtained resistivity curves shown in Fig. 4(b) demonstrate again how sensitive the electric properties are to slight changes in Sb content or defect concentration. The obtained curves cover nearly the whole range of resistivity curves reported in the literature,[4,19,28,29] as already mentioned for films deposited at elevated temperatures. Both samples annealed at 500 °C exhibit, for instance, the same composition within the error bars; nevertheless, their resistivity curves are quite different. Therefore, it has to be guaranteed for possible applications with a usual working temperature of about 500 °C that the composition or the defect concentration does not change during thermal cycling.[40]

Additionally, the intrinsic properties such as bandgap width and conduction mechanisms were investigated. By plotting $\ln \rho$ over $1/T$, the linear regression around 200 K reveals a larger slope for samples annealed at higher temperatures. The corresponding energy gap for an annealing temperature of 300 °C is in the range of 3 meV−4 meV and for 500 °C in the range of 8 meV. These values might not correspond to intrinsic excitation and could be an indication for degeneration or for the formation of subbands. The excitation energy might therefore correspond to an impurity band, as stated for the samples deposited at elevated temperatures. Since the samples annealed at 500 °C exhibit a lower defect concentration than the samples annealed at 300 °C, the charge carrier concentration in the impurity band is also lower resulting in a higher excitation energy.[31,32] The samples deposited at elevated temperatures have the lowest number of defects and thus the highest excitation energy of 20 meV. Nevertheless, the linear dependence and the obtained values have to be confirmed by additional high temperature measurements, as already stated for the samples deposited at elevated temperatures.

At low temperatures, VRH can be determined as dominant conduction mechanism, which is also in agreement with the results obtained for films deposited at elevated temperatures. For annealed films with an Sb content close to 75 at. %, VRH can be found up to ∼30 K for a post-annealing temperature of 300 °C and up to ∼74 K for 500 °C (not shown). These values are lower than the transition temperatures of the films deposited at elevated temperatures, indicating again a higher defect concentration.

### C. Bipolar conduction and controlled doping of $CoSb_3$

The measured room temperature transport coefficients, and especially the discrepancy between the sign of the Seebeck coefficient and the Hall constant, are a result of the complex band structure of $CoSb_3$. A detailed discussion of the individual bands and impurity bands, as well as their contribution to the transport properties, is given by Kajikawa.[31,41] It is shown that the different signs result from the higher mobility of the holes compared to electrons in the system and the different contribution of specific bands to $S$ and $R_H$ at specific temperatures.

To get a simplified picture on how the contribution of different bands of $CoSb_3$ can result in the opposite sign of $R_H$ and $S$, a two band model using the constant effective transport parameters (charge carrier density, mobility) for electrons and holes, respectively, can be used. The Hall constant is then calculated by

$$R_H = \frac{n_p \mu_p^2 - n_e \mu_n^2}{e(n_p \mu_p + n_n \mu_n)^2}.$$

If comparable scattering times are assumed, the effective hole mobility ($\mu_p$) of $CoSb_3$ is larger than the mobility of electrons ($\mu_n$), which is due to the ratio of the effective masses of electrons and holes derived from the band structure.[41,42] Therefore, the ratio of both mobilities was chosen as $\mu_p = 5\mu_n$. Additionally, it is assumed that the hole concentration is in the same range as the electron concentration. From the experimentally determined Hall constants, an average effective charge carrier density of $\sim 10^{20}\,\mathrm{cm}^{-3}$ could be calculated by using the general expression $\overline{R_H} = 1/ne$ of the single band model. This value was used as the initial electron concentration $n_{n0}$ and could be caused by intrinsic properties of the band structure or by doping due to a non-stoichiometric Sb content.

The Hall constant $R_H$ was calculated with these assumptions and is shown in Fig. 5(a) as a function of the hole density $n_p$. The typical dependence with a maximum close to the compensation point of the electrons and the holes ($R_H = 0$), and convergence towards 0 for infinite values of $n_p$ is

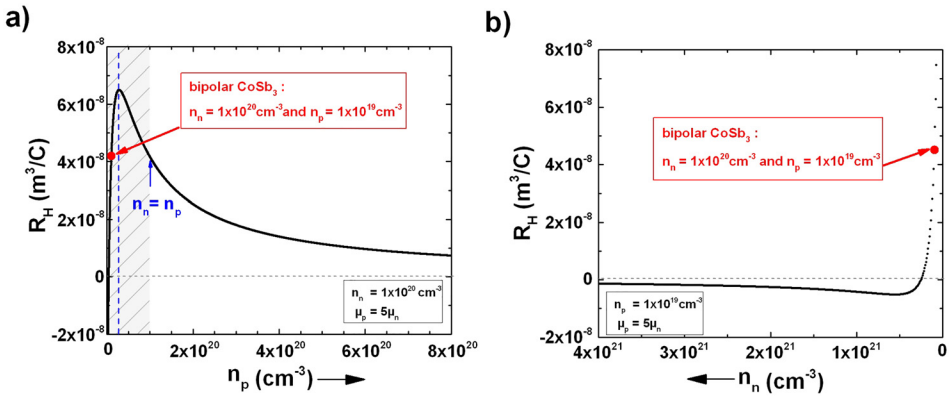


FIG. 5. Calculated Hall constant $R_H$ for Co-Sb thin films showing bipolar conduction. The initial electron density was assumed to be $n_{n0} = 10^{20}\,\mathrm{cm}^{-3}$ and the initial hole density $n_{p0} = 10^{19}\,\mathrm{cm}^{-3}$. The corresponding $R_H$ is marked by the red dot. (a) Change in $R_H$ for various $n_p$ values (p-type doping) and constant $n_n = n_{n0}$; (b) change in $R_H$ for various $n_n$ values (n-type doping) and constant $n_p = n_{p0}$.

obtained. Due to the larger hole mobility, the Hall constant can be positive, even though the electron density is larger than the intrinsic hole density. This range is marked in Fig. 5(a) by the gray shadowed background. The Seebeck coefficient should be negative in this range, since the majority of charge carriers usually dictate the sign of the Seebeck coefficient. However, in the present case, the change from the negative to positive Seebeck coefficient does not occur at the point, where the charge carrier density is equal for both carrier types (also marked in Fig. 5(a)). For the bipolar case, the Seebeck coefficient can be expressed by[43,44]

$$S = \frac{\sigma_p}{\sigma} S_p - \frac{\sigma_n}{\sigma} S_n = \frac{e n_p \mu_p}{\sigma} S_p - \frac{e n_n \mu_n}{\sigma} S_n,$$

with the overall electric conductivity $\sigma = 1/\rho = en\mu$, the electron/hole contribution to the conductivity $\sigma_p/\sigma_n$, and the individual band Seebeck coefficients $S_n$ and $S_p$ related to the corresponding bands with electron and hole conduction, respectively. Thus, the Seebeck coefficient $S$ depends on the bipolar regime linearly on $\mu$, while the Hall constant shows a quadratic dependence. From the equation, it follows that the Seebeck coefficient changes its sign if $n_p\mu_p S_p = n_n\mu_n S_n$. It is further known from the band structure and thermoelectric measurements of bulk samples that $S_n > S_p$.[11,45] By additionally using the above made assumptions, $\mu_p = 5\mu_n$ and $n_n = 10^{20}\,\mathrm{cm}^{-3}$, it can be estimated that the change of sign occurs in that case for hole densities larger than $n_p = n_n/5 = 2 \times 10^{19}\,\mathrm{cm}^{-3}$ (vertical blue dashed line in Fig. 5(a)). Beyond this point, the conductance will be dominated by holes (Seebeck and Hall constant positive), which results in improved thermoelectric properties by a further increase of $n_p$. The p-dominated regime can be realized by p-type doping, for instance, by substituting Co with Fe.

To investigate the influence of p-type doping experimentally, 40-nm-thick $Fe_xCo_{1-x}Sb_3$ thin films with various Fe content ($0 < x < 0.5$) were prepared by codeposition at room temperature followed by post-annealing at 450 °C. The composition was checked by RBS and the successful substitution by XRD combined with Rietveld refinement.[46] The Hall constant of these films was determined and is shown in Fig. 6(a) in dependence of the Fe content $x$. The obtained data agree with the expected curve shown in Fig. 5(a) and

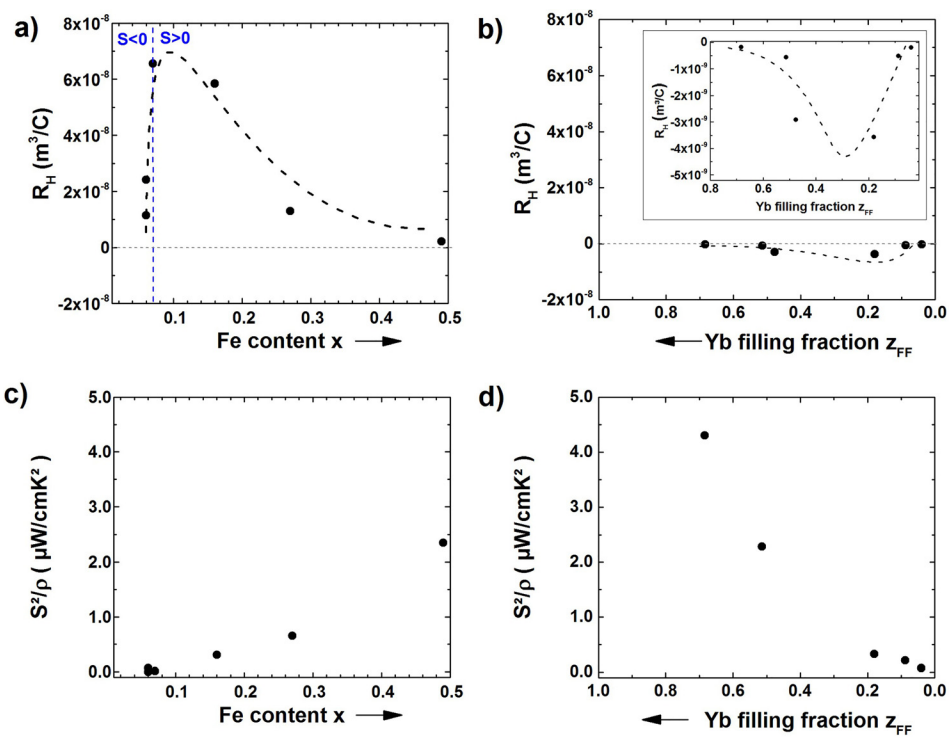


FIG. 6. Experimental investigation of the Hall constant $R_H$ and the power factor $S^2/\sigma$: (a) and (c): For p-type doping of a $CoSb_3$ film by substitution of Co by Fe ($Fe_xCo_{1-x}Sb_3$). $x$ is the corresponding Fe content determined by RBS. (b) and (d) For n-type doping by filling the voids of the $CoSb_3$ lattice structure with Yb ($Yb_{z_{FF}}(CoSb_3)_4$). $z_{FF}$ corresponds to the filling fraction. The inset in (b) reveals more details.

also a change of sign of the Seebeck coefficient was found,[46] which is a proof for the bipolarity of the $CoSb_3$ films. Additionally, the corresponding power factor $S^2/\sigma$ of the Fe doped films is shown in Figure 5(c) to confirm the improved thermoelectric properties in case of p-dominated samples.

Based on the discussed theoretical and experimental results, the initial charge carrier concentrations of the undoped $CoSb_3$ films were defined as $n_{n0} \sim 10^{20}\,cm^{-3}$ and $n_{p0} \sim 10^{19}\,cm^{-3}$. Analog to the p-type doping, the n-type doping was calculated by using $n_{p0} \sim 10^{20}\,cm^{-3}$ and varying $n_n$. It can be seen in Fig. 5(b) that the curve exhibits the expected minimum, but also that much lower absolute values are observed. Note that the scale of the x-axis is changed, and therefore, a much slower convergence is obtained than for p-type doping.

The obtained results were also verified experimentally by n-type doping of $CoSb_3$ films. The electron density $n_n$ is, for instance, increased for non-stoichiometric samples with an Sb content deviating from 75 at. %. However, in our study, all non-stoichiometric single phase skutterudite films reveal a positive Hall constant, and thus, the increase of $n_n$ by compositional changes is not enough to compensate the intrinsic $n_p$. Another way for n-type doping is given by filling of voids in the skutterudite host lattice by guest ions. In our study, n-type doping was achieved by filling $CoSb_3$ with Yb. Therefore, 40-nm-thick $Yb_{z_{FF}}(CoSb_3)_4$ thin films with various filling fraction, $0 < z_{FF} < 0.68$, were prepared by codeposition at room temperature followed by post-annealing at 300 °C.[5] A successful filling was confirmed by XRD combined with a Rietveld refinement (not shown). The measured Hall constant is shown in Fig. 6(b) in dependence of the filling fraction $z_{FF}$, and it is in good agreement to the above discussed differences between $R_H$ for p- and n-type doping. Furthermore, an improvement of the thermoelectric properties is observed as indicated by the determined power factors $S^2/\sigma$ shown in Fig. 6(d).

However, it should be pointed out that the used simplified two band model, although revealing a good starting point how different bands interact with respect to the transport parameters, has to be treated with care. The used formulas for $R_H$ and $S$ have to be extended for all contributing bands, and the charge-neutrality condition has to be fulfilled as discussed in detail by Kajikawa.[41] This allows finally to calculate the absolute values, temperature dependencies, and also the detailed curve shape of the transport parameter in dependence of different doping over a wide range.

## IV. CONCLUSION

In this study, the thermoelectric properties of $CoSb_3$ thin films deposited on $SiO_2$(100 nm)/Si(100) substrates were investigated in dependence of the Sb content. For both investigated preparation methods, (i) deposition on heated substrates and (ii) deposition at room temperature followed by post-annealing, bipolar conduction was found, which leads to poor power factors. While the resistivity is mainly influenced by the exact Sb content of the film, the absolute Seebeck coefficient is increased for single phase skutterudite films. Temperature dependent resistivity measurements revealed a negative temperature coefficient typical for semiconductors and variable range hopping as conduction mechanism at low temperatures. The results also show a very strong influence of small changes in the Sb content on the electric properties at low temperatures, which demands a stable Sb content of the films during heat cycling in the final thermoelectric devices. The positive Hall constant in combination with the negative Seebeck coefficient can be explained with the complex band structure of $CoSb_3$, and it also confirms the larger mobility of holes compared to electrons in this system. Furthermore, p- and n-type doped samples could be produced by doping with Fe or Yb, which give the opportunity to reach the p-dominated ($R_H$ and $S$ positive) or the n-dominated regime ($R_H$ and $S$ negative), where larger power factors are obtained.

## ACKNOWLEDGMENTS

The authors thank the German Research Foundation (DFG) for funding this work via the priority program SPP 1386 "Nanostructured thermoelectrics." We would also like to thank the Helmholtz-Zentrum Dresden-Rossendorf (Germany) for RBS measurements and especially R. Wilhelm for his scientific support.

[1]G. A. Slack, in *CRC Handbook of Thermoelectrics*, edited by D. M. Rowe (CRC Press, 1995).
[2]G. A. Slack and V. Tsoukala, J. Appl. Phys. **76**, 1665 (1994).
[3]G. S. Nolas, D. T. Morelli, and T. M. Tritt, Annu. Rev. Mater. Sci. **29**, 89 (1999).
[4]A. Suzuki, Jpn. J. Appl. Phys., Part 1 **42**, 2843 (2003).
[5]C. He, M. Daniel, M. Grossmann, O. Ristow, D. Brick, M. Schubert, M. Albrecht, and T. Dekorsy, Phys. Rev. B **89**, 174303 (2014).
[6]Z. Zheng, P. Fan, Y. Zhang, J. Luo, Y. Huang, and G. Liang, J. Alloys Compd. **639**, 74 (2015).
[7]S. Katsuyama, Y. Shichijo, M. Ito, K. Majima, and H. Nagai, J. Appl. Phys. **84**, 6708 (1998).
[8]G. Rogl, A. Grytsiv, E. Bauer, P. Rogl, and M. Zehetbauer, Intermetallics **18**, 394 (2010).
[9]D. Mandrus, A. Migliori, T. W. Darling, M. F. Hundley, E. J. Peterson, and J. D. Thompson, Phys. Rev. B **52**, 4926 (1995).
[10]D. T. Morelli, T. Caillat, J.-P. Fleurial, A. Borshchevsky, J. Vandersande, B. Chen, and C. Uher, Phys. Rev. B **51**, 9622 (1995).
[11]T. Caillat, A. Borshchevsky, and J.-P. Fleurial, J. Appl. Phys. **80**, 4442 (1996).
[12]G. Rogl, D. Setman, E. Schafler, J. Horky, M. Kerber, M. Zehetbauer, M. Falmbigl, P. Rogl, E. Royanian, and E. Bauer, Acta Mater. **60**, 2146 (2012).
[13]H. Anno, T. Sakakibara, Y. Notohara, H. Tashiro, T. Koyanagi, H. Kaneko, and K. Matsubara, in *Proceedings of the 16th International Conference on Thermoelectrics (ICT)* (IEEE, 1997), p. 338.
[14]M. S. Dresselhaus, G. Chen, M. Y. Tang, R. Yang, H. Lee, D. Wang, Z. Ren, J.-P. Fleurial, and P. Gogna, Adv. Mater. **19**, 1043 (2007).
[15]T. M. Tritt, *Recent Trends in Thermoelectric Materials Research III* (Gulf Professional Publishing, 2001).
[16]R. Venkatasubramanian, E. Siivola, T. Colpitts, and B. O'Quinn, Nature **413**, 597 (2001).
[17]J. M. O. Zide, D. Vashae, Z. X. Bian, G. Zeng, J. E. Bowers, A. Shakouri, and A. C. Gossard, Phys. Rev. B **74**, 205335 (2006).
[18]A. L. E. Smalley, S. Kim, and D. C. Johnson, Chem. Mater. **15**, 3847 (2003).
[19]V. Savchuk, A. Boulouz, S. Chakraborty, J. Schumann, and H. Vinzelberg, J. Phys. D: Appl. Phys. **92**, 5319 (2002).
[20]S. R. S. Kumar, D. Cha, and H. N. Alshareef, J. Appl. Phys. **110**, 083710 (2011).
[21]A. Möchel, I. Sergueev, N. Nguyen, G. J. Long, F. Grandjean, D. C. Johnson, and R. P. Hermann, Phys. Rev. B. **84**, 064302 (2011).

[22]M. V. Daniel, L. Hammerschmidt, C. Schmidt, F. Timmermann, J. Franke, N. Jöhrmann, M. Hietschold, D. C. Johnson, B. Paulus, and M. Albrecht, Phys. Rev. B **91**, 085410 (2015).
[23]M. V. Daniel, C. Brombacher, G. Beddies, N. Jöhrmann, M. Hietschold, D. C. Johnson, Z. Aabdin, N. Peranio, O. Eibl, and M. Albrecht, J. Alloys Compd. **624**, 216 (2015).
[24]E. Compans, Rev. Sci. Instrum. **60**, 2715 (1989).
[25]R. Bentley, *Theory and Practice of Thermoelectric Thermometry*, Handbook of Temperature Measure Vol. 3 (Springer Verlag, Singapore, 1998).
[26]W.-S. Liu, B.-P. Zhang, J.-F. Li, and L.-D. Zhao, J. Phys. D: Appl. Phys. **40**, 6784 (2007).
[27]H. Kitagawa, M. Wakatsuki, H. Nagaoka, H. Noguchi, Y. Isoda, K. Hasezaki, and Y. Noda, J. Phys. Chem. Solids **66**, 1635 (2005).
[28]S. R. S. Kumar, A. Alyamani, J. W. Graff, T. M. Tritt, and H. N. Alshareef, J. Mater. Res. **26**, 1836 (2011).
[29]H. Anno, K. Matsubara, Y. Notohara, T. Sakakibara, K. Kishimoto, and T. Koyanagi, in *Proceedings of the 15th International Conference on Thermoelectrics (ICT)* (IEEE, 1996), p. 435.
[30]J. S. Dyck, W. Chen, J. Yang, G. P. Meisner, and C. Uher, Phys. Rev. B **65**, 115204 (2002).
[31]Y. Kajikawa, J. Appl. Phys. **116**, 153710 (2014).
[32]Y. Kajikawa, J. Appl. Phys. **116**, 189901 (2014).
[33]H. Ibach and H. Lüth, *Festkörperphysik: Einführung in die Grundlagen*, 7th ed. (Springer-Verlag, Berlin, Heidelberg, 2009).
[34]S. Schuler, "Transporteigenschaften und Defekte in polykristallinen $CuGaSe_2$-Schichten und Heterostrukturen," Ph.D. Dissertation (FU Berlin, 2002).
[35]B. T. Rissom, "Elektrische Transporteigenschaften von epitaktischen und polykristallinen Chalkopyrit-Schichten," Ph.D. Dissertation (FU Berlin, 2007).
[36]P. Sun, B. Wei, J. Zhang, J. M. Tomczak, A. Strydom, M. Søndergaard, B. B. Iversen, and F. Steglich, Nat. Commun. **6**, 7475 (2015).
[37]J. Zhang, W. Cui, M. Juda, D. McCammon, R. L. Kelley, S. H. Moseley, C. K. Stahle, and A. E. Szymkowiak, Phys. Rev. B **48**, 2312 (1993).
[38]A. F. Qasrawi, Cryst. Res. Techol. **37**, 378 (2002).
[39]B. Schüpp, I. Bächer, M. Hecker, N. Mattern, V. Savchuk, and J. Schumann, Thin Solid films **434**, 75 (2003).
[40]M. V. Daniel, M. Friedemann, J. Franke, and M. Albrecht, Thin Solid Films **589**, 203 (2015).
[41]Y. Kajikawa, J. Alloys Compd. **664**, 338 (2016).
[42]J. O. Sofo and G. D. Mahan, Phys. Rev. B **58**, 15620 (1998).
[43]I. Pallecchi, G. Lamura, M. Tropeano, M. Putti, R. Viennois, E. Giannini, and D. V. der Marel, Phys. Rev. B **80**, 214511 (2009).
[44]A. J. Crocker and L. M. Rogers, Br. J. Appl. Phys. **18**, 563 (1967).
[45]D. J. Singh and E. Pickett, Phys. Rev. B **50**, 11235 (1994).
[46]N. Peranio, O. Eibl, S. Bäßler, K. Nielsch, B. Klobes, R. P. Hermann, M. Daniel, M. Albrecht, H. Görlitz, V. Pacheco, N. Bedoya-Martinez, A. Hashibon, and C. Elsässer, Phys. Status Solidi A **213**, 739 (2016).